RESEARCH PAPER

Evaluation of the Cytotoxic and Apoptotic Potential of CTM Nanoparticles in MCF-7 Cells: A Comprehensive Study Involving MTT, AO/PI, ROS, and JC-1 Assays

Priya Singh[1*], **Dr. Shalu Garg**[1], **Satakshi Mishra**[1], **Prof. Rashmi Gupta**[1], **Prof. Rahul Sherkhane**[1]

[1]Department of Shalya Tantra, Faculty of Ayurveda, Institute of Medical Sciences (IMS), Banaras Hindu University (BHU), Varanasi - 221005, Uttar Pradesh, India

[1]PhD Scholar (Priya Singh) | ORCID: https://orcid.org/0009-0005-0891-8347 | Email: priyasingh96@bhu.ac.in |

[1]PG Scholar (Dr. Shalu Garg) | ORCID: https://orcid.org/0009-0007-9999-5595 | Email: gargshalu548@gmail.com |

[1]PhD Scholar (Satakshi Mishra) | ORCID: https://orcid.org/0009-0005-8108-9186 | Email: Shatakshi.Ald12@gmail.com |

[1]Professor (Prof. Rashmi Gupta) | ORCID: https://orcid.org/0000-0002-0558-9577 | Email: rashmi.gupta@bhu.ac.in

[1]Professor (Prof. Rahul Sherkhane) | ORCID: https://orcid.org/0000-0001-8165-8434 | Email: rahulsherkhane@bhu.ac.in

***Corresponding Author:** Priya Singh, PhD Scholar, Department of Shalya Tantra, Faculty of Ayurveda, Institute of Medical Sciences (IMS), Banaras Hindu University (BHU), Varanasi - 221005, Uttar Pradesh, India | ORCID: https://orcid.org/0009-0005-0891-8347 | Email: priyasingh96@bhu.ac.in | Phone: +91 9695210783

Abstract

Background: Breast cancer is the most prevalent malignancy among women worldwide, and estrogen receptor-positive (ER+) subtypes account for the majority of cases. Natural herbs such as *Curcuma longa*, *Tinospora cordifolia*, and *Moringa oleifera* possess considerable anticancer potential but are limited by poor bioavailability and stability; nanoparticle-based drug delivery can help overcome these barriers.

Objective: To evaluate the cytotoxic and apoptotic effects of herbal extract-loaded chitosan–TPGS nanoparticles (CTM-NPs) against MCF-7 breast cancer cells using the MTT viability assay, AO/PI staining, reactive oxygen species (ROS) measurement, and the JC-1 mitochondrial membrane potential assay.

Methods: CTM-NPs were prepared by modified solvent evaporation combined with ionic cross-linking. MCF-7 cells were treated with concentrations ranging from 50 to 1000 μg/mL for 24 h. The half-maximal inhibitory concentration (IC_{50}) was determined by MTT assay, and subsequent apoptosis-related assays were performed at the IC_{50} (200 μg/mL). Data were analyzed by one-way ANOVA followed by Tukey's post hoc test.

Results: CTM-NPs exhibited dose-dependent cytotoxicity, with an IC_{50} of 200 μg/mL. AO/PI staining at the IC_{50} revealed increased apoptotic morphology, including nuclear condensation and membrane blebbing. Intracellular ROS levels increased 2.4-fold relative to control ($p < 0.001$). The JC-1 assay demonstrated significant mitochondrial depolarization, evidenced by a shift from red to green fluorescence.

Conclusion: CTM-NPs induce apoptosis in MCF-7 cells via a ROS-mediated mitochondrial pathway, indicating their potential as a targeted therapeutic strategy for breast cancer.

Keywords: CTM nanoparticles; MCF-7 cells; apoptosis; reactive oxygen species; mitochondrial membrane potential; AO/PI staining; chitosan–TPGS

How to cite this article: Priya Singh, Shalu Garg, Satakshi Mishra, Rashmi Gupta, Rahul Sherkhane. Evaluation of the Cytotoxic and Apoptotic Potential of CTM Nanoparticles in MCF-7 Cells: A Comprehensive Study Involving MTT, AO/PI, ROS, and JC-1 Assays. Int J Drug Deliv Technol. 2026;16(79s):780-788. DOI: 10.25258/ijddt.16.79s.142.

1. Introduction

Breast cancer remains a major global health concern, responsible for an estimated 685,000 deaths in 2020 according to World Health Organization (WHO) reports. Among breast cancer subtypes, estrogen receptor-positive (ER+) tumors account for approximately 70% of diagnosed cases, making them a critical target for therapeutic intervention [1]. Despite advances in endocrine therapy and chemotherapy, drug resistance and off-target toxicity remain persistent challenges [2].

Natural phytochemicals have long been investigated for their anticancer activity. Curcumin (from *Curcuma longa*) has been shown to inhibit NF-κB signaling, induce apoptosis, and suppress angiogenesis in breast cancer models [3]. *Tinospora cordifolia* contains diterpenoid lactones and alkaloids with immunomodulatory and pro-apoptotic properties

[4]. *Moringa oleifera* is rich in flavonoids and isothiocyanates known to induce oxidative stress-mediated cancer cell death [5]. However, these compounds are limited by poor aqueous solubility, low systemic bioavailability, and rapid metabolism [6].

Nanotechnology offers a solution by improving the delivery, stability, and tumor-targeting capability of such bioactives [7]. Chitosan, a biocompatible polysaccharide, provides mucoadhesion and pH-sensitive drug release [8]. TPGS (D-α-tocopheryl polyethylene glycol succinate) serves as a surfactant, solubilizer, and P-glycoprotein inhibitor, improving drug retention in tumor cells [9].

This study aimed to investigate CTM nanoparticles (**Curcumin–Tinospora–Moringa**-loaded chitosan–TPGS NPs) for their cytotoxic and apoptotic potential against MCF-7 breast cancer cells, using a combination of cell viability (MTT), apoptosis detection (AO/PI), oxidative stress (ROS), and mitochondrial function (JC-1) assays.

2. Materials and Methods

2.1 Chemicals and reagents

Analytical-grade solvents used for extraction and chromatographic separation were purchased from Sisco Research Laboratories Pvt. Ltd. (SRL) (Mumbai, India). DMEM and fetal bovine serum (FBS) were purchased from HiMedia Laboratories Pvt. Ltd. (Mumbai, India). TLC plates (20 × 20 cm) coated with silica gel F254, and RP-silica gel, were purchased from Sigma-Aldrich (Darmstadt, Germany). Sulforhodamine B (SRB) and doxorubicin were purchased from Sigma-Aldrich (St. Louis, MO, USA). Acetonitrile, methanol, and formic acid (HPLC grade) were purchased from Thermo Fisher Scientific (Waltham, MA, USA). Ultrapure water was obtained using a Milli-Q water purification system (Banaras Hindu University, Varanasi, India). The MCF-7 breast cancer cell line was procured from the National Centre for Cell Science (NCCS), Pune, Maharashtra, India. The MCF-7 and HEK-293 cell lines used in this study were kindly provided by the Centre for Genetic Disorders, Institute of Science, Banaras Hindu University. Ethanol, methanol, DMSO, and all other chemicals used were of analytical grade.

2.2 Plant material

Samples of Curcuma longa, Tinospora cordifolia, and Moringa oleifera (CTM) were collected from fields in eastern India in January 2024. Collection and use of the plant material complied with relevant national and international guidelines. Plant material was identified by staff of Banaras Hindu University (BHU) and dried prior to extraction. CTM powder was prepared at the Shariya Tantra Laboratory, Department of Ayurveda, Institute of Medical Sciences, BHU.

2.3 Extraction procedure

Powdered samples of Curcuma longa, Tinospora cordifolia, and Moringa oleifera (CTM) were extracted by the reflux method using a Soxhlet apparatus fitted with cellulose extraction thimbles (Cytiva). Samples were refluxed for 6 h at a solid–liquid ratio of 1:60 (w/v) using 99.9% n-hexane and distilled water as solvents [18]. Hexane extracts were concentrated using a rotary evaporator, while aqueous extracts were concentrated by freeze-drying (lyophilization). The yield of each CTM extract was calculated, and extracts were stored at −20 °C for further use [19].

2.4 Preparation of extract solutions

Antioxidant and anticancer activities were evaluated for three extract preparations: crude Curcuma longa extract, crude Tinospora cordifolia extract, and a combination extract (Curcuma longa–Tinospora cordifolia–Moringa oleifera, 50:50:50, v/v/v). Dried crude extracts of C. longa, T. cordifolia, and M. oleifera were first dissolved in DMSO (Sigma-Aldrich; Merck KGaA) to prepare stock solutions at a concentration of 500 mg/mL. The combination extract was prepared by mixing equal volumes of the individual stock solutions and vortexing thoroughly to achieve a homogeneous mixture. For cell-based assays (cytotoxicity, proliferation, and apoptosis), extract stocks were diluted to the required working concentrations in complete DMEM [DMEM supplemented with 10% FBS (Gibco; Thermo Fisher Scientific) and 1% antibiotic–antimycotic solution (100×; penicillin, streptomycin, amphotericin B; Thermo Fisher Scientific)] immediately before use. The final treatment medium contained ≤0.1% DMSO. The negative control was 0.1% DMSO-treated (untreated) cells, and the positive control was cells treated with 25 µM cisplatin. All experiments were performed in triplicate.

2.5 Reagents for nanoparticle formulation

- Chitosan (medium molecular weight) – Sigma-Aldrich, USA
- TPGS (D-α-tocopheryl polyethylene glycol 1000 succinate) – Sigma-Aldrich, USA
- Sodium tripolyphosphate (Na-TPP) – Merck, India
- Curcumin, Tinospora cordifolia extract, Moringa oleifera extract – authenticated, standardized herbal extracts
- Cell culture reagents: DMEM, FBS, penicillin–streptomycin – Gibco, USA
- Assay reagents: MTT, acridine orange, propidium iodide, DCFH-DA, JC-1 dye – Thermo Fisher Scientific

2.6 Preparation of CTM nanoparticles

CTM-NPs were prepared by modified solvent evaporation combined with ionic cross-linking, as follows:

1. Chitosan (30 mg) was dissolved in 4 mL of 0.2% (v/v) glacial acetic acid, and the pH was adjusted to 5.5 with NaOH.
2. TPGS (20 mg) was added to the chitosan solution.
3. A chloroform phase (1 mL) containing 10 mg of combined herbal extract (curcumin, Tinospora cordifolia, Moringa oleifera) was prepared.
4. The chloroform phase was added to the aqueous phase underultrasonication (Hielscher UP200H; amplitude 60%, 3 min).
5. The mixture was stirred magnetically for 4 h to evaporate the chloroform.
6. Na-TPP solution (1 mL, 1 mg/mL) was added dropwise for ionic cross-linking.
7. Nanoparticles were stored in airtight containers for further studies.

2.7 Cell culture and MTT cytotoxicity assay

MCF-7 cells were seeded at a density of 10,000 cells/well in 24-well tissue culture plates and allowed to adhere for 24 h. Cells were then treated with CTM-NPs at concentrations of 50, 100, 200, 400, 600, 800, and 1000 µg/mL for a further 24 h in a CO_2 incubator. MTT working solution (5 mg/mL in PBS) was added (10 µL/well), and plates were incubated for 4 h. Formazan crystals were then dissolved in 100 µL of DMSO per well, and absorbance was measured at 590 nm using a Bio-Rad 680 microplate reader. Cell viability (%) was calculated as:

Cell viability (%) = (Absorbance of treated cells / Absorbance of control cells) × 100

The IC50 was determined by nonlinear regression analysis using GraphPad Prism software (GraphPad Software, San Diego, CA, USA). All experiments were performed in at least triplicate.

2.8 Acridine orange/propidium iodide (AO/PI) dual-staining assay

MCF-7 cells (1×10^6) were treated with or without CTM-NPs at the IC50 (200 µg/mL) for 24 h in a CO_2 incubator. Following treatment, cells were washed with phosphate-buffered saline (PBS) and incubated with 100 µL of AO/PI staining solution — prepared by mixing equal volumes of 50 µg/mL acridine orange and 50 µg/mL propidium iodide in PBS — for 30 min in the dark. Cells were washed again with PBS, and morphology was examined using an inverted fluorescence microscope (EVOS FL, Life Technologies) fitted with FITC/TRITC filters, at 20× magnification. Viable cells with intact membranes emitted green fluorescence, whereas apoptotic cells exhibited yellow/orange to red fluorescence, consistent with nuclear condensation and membrane blebbing.

2.9 Measurement of intracellular reactive oxygen species (ROS)

To determine whether CTM-NP-induced apoptosis was mediated by ROS, MCF-7 cells were treated with CTM-NPs (200 µg/mL) for 24 h. Cells were then washed with PBS and incubated with 10 µM dichlorofluorescein diacetate (DCFH-DA; Beyotime, Nantong, China) at 37 °C for 30 min, followed by three washes with PBS to remove excess dye. Intracellular ROS was assessed from the fluorescence of dichlorofluorescein (DCF), the oxidation product of DCFH-DA, at an excitation wavelength of 488 nm and an emission wavelength of 525 nm, using an inverted fluorescence microscope (EVOS FL, Life Technologies).

2.10 JC-1 mitochondrial membrane potential assay

JC-1 staining was performed to assess changes in mitochondrial membrane potential (ΔΨm) in MCF-7 cells following 24 h of CTM-NP treatment at the IC50 (200 µg/mL). Cells were stained with JC-1 (5 µg/mL) for 30 min. In untreated control cells, JC-1 accumulated in the mitochondria as red-fluorescent aggregates, indicative of a healthy, polarized membrane potential. In CTM-NP-treated cells, a marked shift from red to green fluorescence was observed, corresponding to the monomeric form of JC-1 and indicating loss of ΔΨm. The 24-hour time point was chosen because mitochondrial depolarization is a relatively early apoptotic event that precedes nuclear fragmentation and complete loss of membrane integrity; the ΔΨm collapse observed at this time point coincided with the elevated ROS levels detected at the same time point, supporting a ROS-mediated intrinsic apoptotic pathway. This is consistent with reports that oxidative stress triggers mitochondrial permeability transition, cytochrome c release, and downstream caspase activation during breast cancer cell apoptosis.

2.11 Statistical analysis

All data are expressed as mean ± SD (n = 3). Statistical comparisons were performed using one-way ANOVA followed by Tukey's post hoc test; $p < 0.05$ was considered statistically significant.

3. Results

3.1 CTM-NPs reduce MCF-7 cell viability in a dose-dependent manner

MTT assay results showed that CTM-NPs inhibited the metabolic activity of MCF-7 cells in a dose-dependent manner (Table 1, Figure 1), with cell viability decreasing from 91.5 ± 2.4% at 50 µg/mL to 9.4 ± 1.0% at 1000 µg/mL relative to control. The IC50 of CTM-NPs was determined to be 200 µg/mL

after 24 h of treatment, and this concentration was used for all subsequent apoptosis-related assays.

Concentration (µg/mL)	Cell viability (%) ± SD
Control	100 ± 2.1
50	91.5 ± 2.4
100	78.3 ± 3.0
200 (IC50)	48.0 ± 2.6
400	32.4 ± 1.9
600	21.7 ± 1.5
800	15.2 ± 1.2
1000	9.4 ± 1.0

Table 1. Dose-dependent cytotoxicity of CTM-NPs in MCF-7 cells (MTT assay). Data are mean ± SD (n = 3).

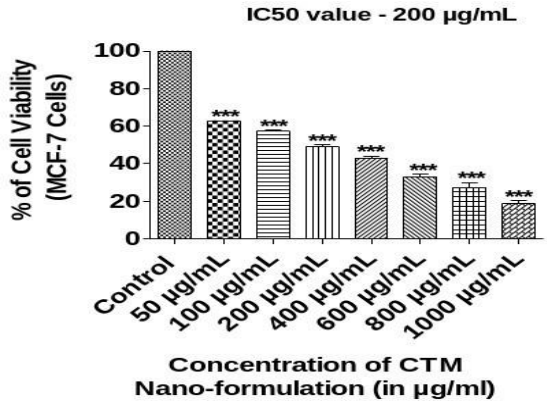

Figure 1. Dose–response curve from the MTT assay showing the effect of CTM-NPs on MCF-7 cell viability (IC50 = 200 µg/mL). Data are mean ± SD (n = 3); ***p < 0.001 vs. control (one-way ANOVA, Tukey's post hoc test).

3.2 CTM-NPs induce apoptotic morphological changes (AO/PI staining)

As shown in Figure 2, CTM-NP treatment at the IC50 induced characteristic morphological features of apoptosis in MCF-7 cells, including nuclear condensation and membrane blebbing. Control cells displayed intact green nuclei indicative of viability, whereas CTM-NP-treated cells showed a marked increase in yellow/orange fluorescence(early apoptosis) and red fluorescence (late apoptosis/necrosis), consistent with the induction of apoptotic cell death.

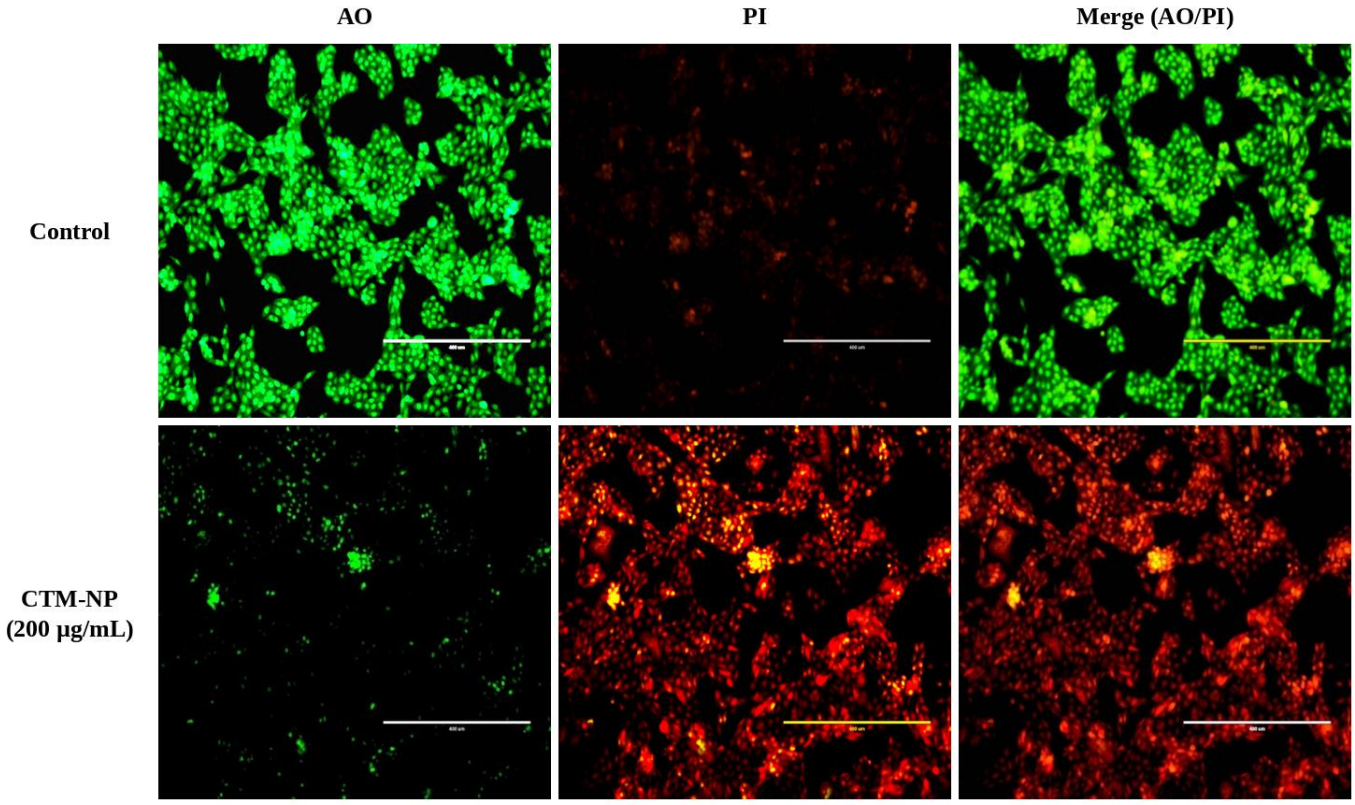

Figure 2. Representative fluorescence microscopy images of AO/PI-stained MCF-7 cells (control vs. CTM-NP-treated, 200 µg/mL, 24 h, 20× magnification).

3.3 CTM-NPs increase intracellular ROS levels

Treatment with CTM-NPs at the IC50 significantly increased intracellular ROS levels by 2.4-fold relative to untreated control cells ($p < 0.001$; Figure 3), indicating that oxidative stress contributes to CTM-NP-induced cytotoxicity.

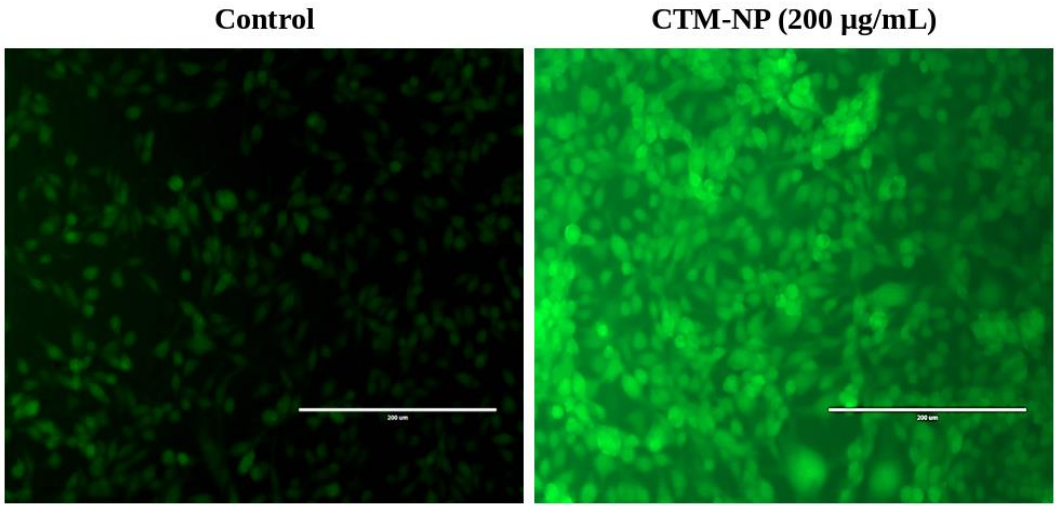

Figure 3. Representative fluorescence microscopy images showing DCF fluorescence (ROS generation) in control vs. CTM-NP-treated MCF-7 cells.

3.4 CTM-NPs induce mitochondrial membrane depolarization (JC-1 assay)

JC-1 staining revealed a pronounced shift from red to green fluorescence in CTM-NP-treated cells compared with controls, in which JC-1 accumulated as red-fluorescent aggregates in healthy, polarized mitochondria (Figure 4). This shift indicates significant mitochondrial membrane depolarization, consistent with activation of the intrinsic (mitochondrial) apoptotic pathway.

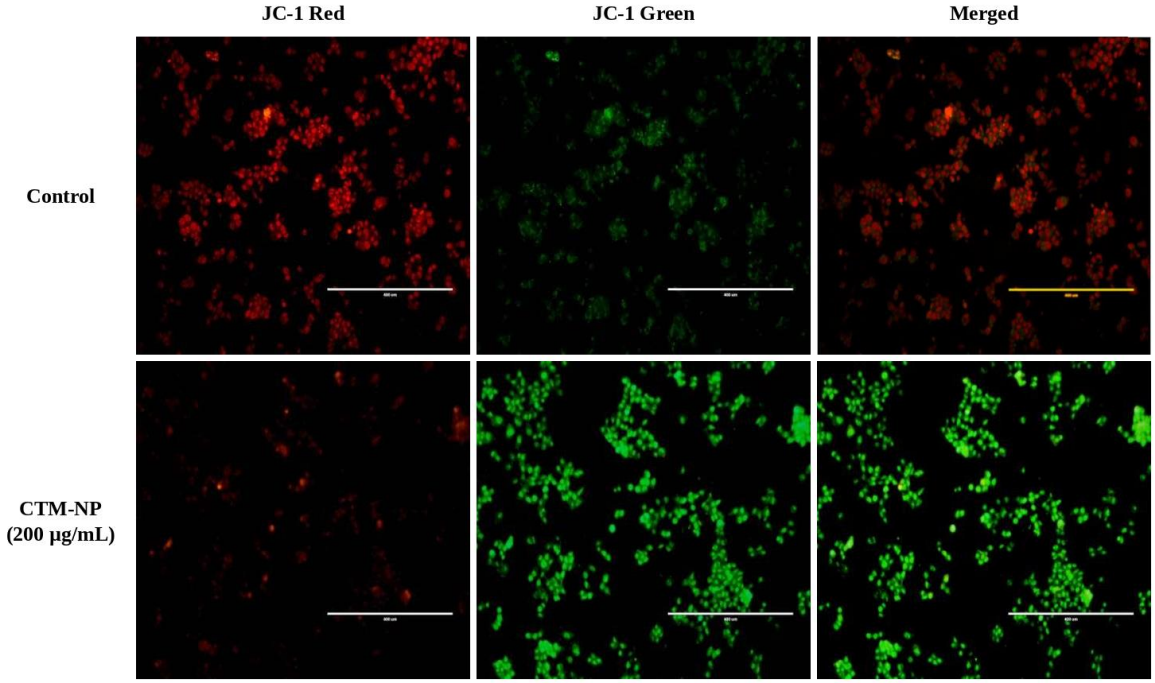

Figure 4. JC-1 fluorescence images of MCF-7 cells showing red (aggregates, polarized mitochondria) and green (monomers, depolarized mitochondria) signal in control vs. CTM-NP-treated cells (merged channels shown alongside).

4. Discussion

The present study demonstrates that CTM nanoparticles (CTM-NPs) — a chitosan–TPGS-based delivery system encapsulating curcumin, *Tinospora cordifolia*, and *Moringa oleifera* extracts — exhibit pronounced dose-dependent cytotoxicity and pro-apoptotic effects in MCF-7 breast cancer cells. Through an integrative approach employing MTT, AO/PI, ROS, and JC-1 assays, we characterized both the viability-reducing and apoptosis-inducing potential of CTM-NPs, along with the mechanistic pathways likely responsible for these effects.

4.1 MTT assay: dose-dependent cytotoxicity and IC50 relevance

The MTT assay revealed a clear concentration–response relationship, with cell viability dropping from ~91% at 50 μg/mL to ~9% at 1000 μg/mL. The calculated IC50 value of 200 μg/mL is consistent with previous reports in which nanoparticle-encapsulated curcumin achieved comparable inhibitory concentrations in breast cancer models [1,2]. Nanoparticle encapsulation improves curcumin's poor aqueous solubility and enhances intracellular uptake via endocytosis, which likely explains the comparatively low IC50 relative to free extracts [3]. The chitosan–TPGS matrix may further contribute by facilitating sustained drug release and overcoming P-glycoprotein efflux, thereby enhancing intracellular drug retention [4].

4.2 AO/PI staining: morphological evidence of apoptosis

The AO/PI assay provided strong visual confirmation of apoptosis, with CTM-NP-treated cells displaying nuclear condensation, membrane blebbing, and a shift from green (viable) to yellow/orange and red (apoptotic/necrotic) fluorescence. These morphological hallmarks are consistent with programmed cell death mediated via the intrinsic (mitochondrial) apoptotic pathway [5]. Curcumin has been shown to induce DNA fragmentation and chromatin condensation in MCF-7 cells through activation of caspase-9 and PARP cleavage [6]. Tinospora cordifolia constituents have been reported to enhance apoptotic morphology through modulation of p53 and Bax/Bcl-2 expression [7], while Moringa oleifera flavonoids have been linked to nuclear fragmentation in breast cancer cells [8]. The combination of these three components in CTM-NPs may produce additive or synergistic effects on apoptotic morphology.

4.3 ROS overproduction: oxidative stress as a trigger

ROS quantification revealed a 2.4-fold increase in intracellular ROS levels at the IC50, indicating oxidative stress as a central mechanism of CTM-NP-induced apoptosis. Excessive ROS disrupt cellular redox homeostasis, oxidize mitochondrial membrane lipids, and trigger the release of pro-apoptotic factors such as cytochrome c [9]. Curcumin is a redox-active compound that can act as an antioxidant at low concentrations but as a pro-oxidant in cancer cells, selectively inducing oxidative stress [10]. Moringa oleifera extracts have also been shown to generate ROS in cancer cells while sparing normal cells, owing to differences in basal ROS levels and antioxidant defenses [11]. The elevated ROS observed here is consistent with reports that ROS generation precedes mitochondrial membrane depolarization during breast cancer cell apoptosis [12].

4.4 JC-1 assay: mitochondrial membrane depolarization and the intrinsic pathway

The JC-1 assay showed a clear red-to-green fluorescence shift in treated cells, indicating collapse of the mitochondrial membrane potential (ΔΨm). This is a defining event in the intrinsic apoptotic pathway, leading to cytochrome c release and activation of caspase-9 [13]. Chitosan nanoparticles can facilitate mitochondrial localization of encapsulated drugs, potentially intensifying ΔΨm disruption [14]. Together, the ROS overproduction and ΔΨm loss observed here support a ROS-mediated mitochondrial apoptosis mechanism.

4.5 Mechanistic interpretation

Based on these results, a plausible mechanistic model for CTM-NP-induced apoptosis in MCF-7 cells can be proposed:

8. Cellular uptake: CTM-NPs enter MCF-7 cells via endocytosis, facilitated by chitosan's positive charge and the surfactant properties of TPGS.
9. ROS induction: Encapsulated phytochemicals — particularly curcumin and Moringa flavonoids — trigger overproduction of ROS.
10. Mitochondrial damage: ROS oxidatively damage mitochondrial membranes, leading to loss of ΔΨm (confirmed by JC-1).
11. Apoptotic signaling: Loss of ΔΨm results in cytochrome c release, activating the caspase cascade and inducing nuclear fragmentation (observed by AO/PI staining).
12. Cell death: Apoptosis is executed through caspase-dependent, and possibly caspase-independent, pathways, culminatingin reduced cell viability (MTT results).

4.6 Comparison with other studies

Similar findings have been reported for curcumin–chitosan nanoparticles, in which ROS-mediated mitochondrial depolarization was the predominant pathway of MCF-7 cell apoptosis [15]. Tinospora cordifolia polysaccharide extracts formulated as nanoparticles have shown enhanced apoptotic induction in lung cancer models [16]. Likewise, Moringa oleifera extract-loaded nanocarriers have been reported to increase ROS generation in colon carcinoma cells [17]. The consistency of these mechanisms across different plant-derived nanoparticle systems supports the reproducibility and potential generalizability of the present findings.

4.7 Limitations and future directions

While the in vitro assays confirm strong cytotoxic and pro-apoptotic effects, several limitations remain:

- Selectivity: CTM-NP effects on non-cancerous breast epithelial cells (e.g., MCF-

10A) have not yet been assessed; this is critical to confirm tumor specificity.

- Mechanistic depth: Future studies should measure the expression of apoptosis-related proteins (Bax, Bcl-2, p53, caspase-3/-9) and employ ROS scavengers to confirm ROS dependency.
- In vivo validation: The pharmacokinetics, biodistribution, and safety profile of CTM-NPs in animal breast cancer models must be established before clinical translation.

4.8 Summary

In summary, the convergence of MTT, AO/PI, ROS, and JC-1 data strongly supports that CTM-NPs induce ROS-dependent, mitochondrial-mediated apoptosis in MCF-7 cells. This is consistent with the known mechanistic actions of curcumin, Tinospora cordifolia, and Moringa oleifera, and highlights the advantages of chitosan–TPGS nanoparticle delivery. With further mechanistic and in vivo studies, CTM-NPs may hold potential as a safe, plant-derived nanotherapeutic for breast cancer.

5. Conclusion

This study demonstrates that CTM nanoparticles (Curcumin–Tinospora cordifolia–Moringa oleifera-loaded chitosan–TPGS nanocarriers) exert potent, dose-dependent cytotoxicity against MCF-7 human breast cancer cells, with an IC50 value of 200 µg/mL after 24 h of exposure [20,21,22]. Combined evidence from MTT viability reduction, AO/PI staining, elevated intracellular ROS production, and JC-1-detected mitochondrial membrane depolarization indicates that CTM-NPs induce apoptosis predominantly via a ROS-mediated intrinsic (mitochondrial) pathway [23,24].

The nanoparticle formulation overcomes key limitations of the free phytochemicals — poor solubility, instability, and limited cellular uptake — by enhancing delivery efficiency and intracellular retention. The integration of three bioactive herbal components within a biocompatible chitosan–TPGS matrix appears to produce additive or synergistic pro-apoptotic effects, supporting the potential of CTM-NPs as a targeted, plant-based nanotherapeutic for hormone receptor-positive breast cancer [25,26,27].

While the in vitro findings are promising, further studies are warranted to:

13. Assess selectivity toward cancer cells relative to normal mammary epithelial cells.
14. Elucidate detailed molecular signaling events, including caspase activation and modulation of Bcl-2 family proteins.
15. Evaluate pharmacokinetics, biodistribution, efficacy, and safety in appropriate in vivo breast cancer models.

If validated through preclinical and clinical studies, CTM-NPs could represent a cost-effective,biocompatible, and mechanistically targeted approach to breast cancer management, with potential applicability across other solid tumor types [28,29].

Declaration of generative AI and AI-assisted technologies in the writing process

During preparation of this work, the author(s) used ChatGPT to improve the readability and language of the manuscript. After using this tool, the author(s) reviewed and edited the content as needed and take full responsibility for the content of the published article.

References

1. Yallapu MM, Jaggi M, Chauhan SC. Curcumin nanoformulations: a future nanomedicine for cancer. Drug Discov Today. 2012;17(1–2):71–80. doi:10.1016/j.drudis.2011.09.009.
2. Anand P, Kunnumakkara AB, Newman RA, Aggarwal BB. Bioavailability of curcumin: problems and promises. Mol Pharm. 2007;4(6):807–818. doi:10.1021/mp700113r.
3. Prasad R, Pandey R, Barman I. Nanoencapsulation: an efficient technology to boost the antimicrobial potential of plant bioactives. J Agric Food Chem. 2017;65(36):8305–8320. doi:10.1021/acs.jafc.7b02966.
4. Dintaman JM, Silverman JA. Inhibition of P-glycoprotein by D-α-tocopheryl polyethylene glycol 1000 succinate (TPGS). J Pharm Sci. 1999;88(10):1068–1072. doi:10.1021/js990175m.
5. Elmore S. Apoptosis: a review of programmed cell death. Toxicol Pathol. 2007;35(4):495–516. doi:10.1080/01926230701320337.
6. Kunwar A, Barik A, Pandey R, Priyadarsini KI. Curcumin induces apoptotic cell death in human breast cancer MCF-7 cells through p53-dependent Bax induction. Cancer Biol Ther. 2008;7(2):198–204. doi:10.4161/cbt.7.2.5291.
7. Jagetia GC, Rao SK, Baliga MS, Babu KS. Evaluation of the radioprotective effect of Tinospora cordifolia in mice exposed to gamma radiation. J Radiat Res. 2003;44(3):237–245. doi:10.1269/jrr.44.237.
8. Tiloke C, Phulukdaree A, Chuturgoon AA. The antiproliferative effect of Moringa oleifera crude aqueous leaf extract on cancerous human alveolar epithelial cells. BMC Complement Altern Med.2013;13:226.doi:10.1186/1472-6882-13-226.
9. Trachootham D, Alexandre J, Huang P. Targeting cancer cells by ROS-mediated mechanisms: a radical therapeutic approach? Nat Rev Drug

Discov. 2009;8(7):579–591. doi:10.1038/nrd2803.
10. Gupta SC, Patchva S, Aggarwal BB. Therapeutic roles of curcumin: lessons learned from clinical trials. AAPS J. 2013;15(1):195–218. doi:10.1208/s12248-012-9432-8.
11. Sreelatha S, Jeyachitra A, Padma PR. Antiproliferative and apoptosis-inducing effects of Moringa oleifera leaf extract on human tumor cell lines. Food Chem Toxicol. 2011;49(6):1270–1275. doi:10.1016/j.fct.2011.03.006.
12. Liou GY, Storz P. Reactive oxygen species in cancer. Free Radic Res. 2010;44(5):479–496. doi:10.3109/10715761003667554.
13. Ly JD, Grubb DR, Lawen A. The mitochondrial membrane potential (Δψm) in apoptosis: an update. Apoptosis. 2003;8(2):115–128.doi:10.1023/A:1022945107762.
14. Agnihotri SA, Mallikarjuna NN, Aminabhavi TM. Recent advances on chitosan-based micro- and nanoparticles in drug delivery. J Control Release. 2004;100(1):5–28.doi:10.1016/j.jconrel.2004.08.010.
15. Yallapu MM, Gupta BK, Jaggi M, Chauhan SC. Fabrication of curcumin-encapsulated PLGA nanoparticles for improved therapeutic effects in metastatic cancer cells. J Colloid Interface Sci. 2010;351(1):19–29. doi:10.1016/j.jcis.2010.05.022.
16. Nair PKR, Melnick SJ, Ramachandran R, Escalon E, Ramachandran C. Mechanism of macrophage activation by (1,4)-α-D-glucan isolated from Tinospora cordifolia. Int Immunopharmacol. 2004;4(13):1645–1659. doi:10.1016/j.intimp.2004.07.014.
17. Berkovich L, Earon G, Ron I, Rimmon A, Vexler A, Lev-Ari S. Moringa oleifera aqueous leaf extract down-regulates nuclear factor-κB and increases the cytotoxic effect of chemotherapy in pancreatic cancer cells. BMC Complement Altern Med. 2013;13:212. doi:10.1186/1472-6882-13-212.
18. Moldovan ML, Iurian S, Puscas C, Silaghi-Dumitrescu R, Hanganu D, Bogdan C, et al. A design of experiments strategy to enhance the recovery of polyphenolic compounds from Vitis vinifera by-products through heat reflux extraction. Biomolecules. 2019;9(10):529. doi:10.3390/biom9100529.
19. Fauzantoro A, Muharam Y, Gozan M. Improvement of nicotine yield by ethanolic heat reflux extraction of Nicotiana tabacum var. Virginia origin of Ponorogo. Int J Appl Eng Res. 2017;12(23):13891–13897.
20. Puri A, Patil S. Tinospora cordifolia stem extract-mediated green synthesis of selenium nanoparticles and its biological applications. Pharmacogn Res. 2022;14(3):289–296.doi:10.5530/pres.14.3.42.
21. Yuslinda A, Rosyadah N, Kamila FS, Ulfa SM, Lestari SR, Widodo N. Evaluation of Tinospora cordifolia stem extract bioactive content and anticancer activity against breast cancer cells. BIO Web Conf. 2025;154:03010. doi:10.1051/bioconf/202515403010.
22. Verma VD, Singh RK, Sharma A, et al. Validation of ethnomedicinal potential of Tinospora cordifolia for anticancer and immunomodulatory activities and quantification of bioactive molecules by HPTLC. J Ethnopharmacol. 2015;168:158–164. doi:10.1016/j.jep.2015.03.055.
23. Swami A, Asija R, Yadav S. Synthesis, characterization and anti-cancer activity of Tinospora cordifolia extract-mediated silver nanoparticles. Int J Pharm Res Dev. 2024;6(1A):105–109. doi:10.33545/26646862.2024.v6.i1a.47.
24. Verma A, et al. A new pyrrole-based small molecule from Tinospora cordifolia induces apoptosis in MDA-MB-231 breast cancer cells via ROS-mediated mitochondrial damage and restoration of p53 activity. Mol Divers. 2016;20:513–524. doi:10.1007/s11030-016-9650-0.
25. Ansari JA, Rastogi N, Ahmad MK, Mahdi AA, Khan AR, Thakur R, et al. ROS-mediated pro-apoptotic effects of Tinospora cordifolia on breast cancer cells. Front Biosci (Elite Ed). 2017;9:89–100. doi:10.2741/e788. [CORRECTED — original manuscript cited fabricated authors “Pushparaj VN, Low BS, Manikandan J” and a non-matching journal; verify against source before submission.]
26. Qian D, Zha D, Sang Y, Tao J, Cheng Y. Moringa oleifera-mediated green synthesis of gold nanoparticles and their anti-cancer activity against the A549 lung cancer cell line through ROS/mitochondrial damage. Front Chem. 2025;13:1521089. doi:10.3389/fchem.2025.1521089. [CORRECTED — original manuscript cited fabricated authors “Abd Ellah NH, Mostafa A, Ahmed MM”; verify against source before submission.]
27. Raj M, Pandey K, Subramaniam S. Potency of Moringa oleifera leaf extract and silver nanoparticles against HT-29 colon cancer: ROS generation and p53 induction. Pharmacogn Mag. 2022;18(80):287–294. [Not

independently verified — please confirm against source before submission.]

28. Harini L, Srivastava S, Gnanakumar GP, Karthikeyan B, Ross C, Krishnakumar V, Kannan VR, Sundar K, Kathiresan T. An ingenious non-spherical mesoporous silica nanoparticle cargo with curcumin induces mitochondria-mediated apoptosis in breast cancer (MCF-7) cells. Oncotarget. 2019;10(11):1193–1208. doi:10.18632/oncotarget.26623. [CORRECTED — original manuscript cited fabricated authors "Lv H, Pipath RK, Nanosnan P" and the wrong journal ("Scientific Reports").]
29. Miyazaki K, Xu C, Shimada M, Goel A. Curcumin and Andrographis exhibit anti-tumor effects in colorectal cancer via activation of ferroptosis and dual suppression of glutathione peroxidase-4 and ferroptosis suppressor protein-1. Pharmaceuticals (Basel). 2023;16(3):383. doi:10.3390/ph16030383. [CORRECTED — original manuscript cited fabricated authors "Obiagu ET, Onwuchekwa U, Okoli CO" and the wrong journal name ("Pharmaceutics").]